12 March 1999

ELSEVIER

Chemical Physics Letters 302 (1999) 139–145

CHEMICAL PHYSICS LETTERS

Spectral measurements in production of single-wall carbon nanotubes by laser ablation

Sivaram Arepalli [a], Carl D. Scott [b,*]

[a] *GB Tech, 2200 Space Park Drive, Houston, TX 77058, USA*
[b] *NASA Johnson Space Center, Houston, TX 77058-3696, USA*

Received 12 October 1998; in final form 22 December 1998

Abstract

Measurements are made of optical radiation from the luminous plume in a flow tube used to produce single-wall carbon nanotubes by laser ablation of graphite. Measurements include 10 μs exposures for a spectral region of 310–630 nm taken at several times after single and two-laser pulses and time-dependent measurements at a number of wavelengths. Strong emission from the C_2 Swan bands and possibly from C_3 are seen superimposed on a significant continuum the origin of which is uncertain. Temperatures estimated from ratios of intensities of Swan band features are in the range of 2500–4000 K.

1. Introduction

There has been great interest in the production and characterization of single-wall carbon nanotubes (SWNT) because of possible applications in nanostructures [1], super-strong materials [2], nanoelectronics [3], and hydrogen storage [4]. A variety of processes have been used to produce them, including arcs [5–7], laser ablation [8], chemical vapor deposition [9] (CVD), and pyrolysis [10].

SWNTs are being produced at the NASA Johnson Space Center using the laser ablation process developed at Rice University [8]. Details of the formation of SWNTs are not well understood, but empirical process variations have helped to optimize production rates and nanotube yield and purity. It has been speculated that the growth of nanotubes occurs from partially closed fullerenes held 'open' by nano-sized particles of Co/Ni metal catalyst on which C_2 attaches. A recent study by Yudasaka et al. [11] focused on Raman measurements of SWNTs grown by laser ablation in argon at different pressures. Unfortunately, there have been no known successful attempts to measure directly the formation of SWNTs in situ.

The objective of this work is to measure the evolution of observable C_2 emission from the plume in the ultraviolet and visible region of the spectrum and to infer information about the formation of carbon nanotubes. We will present time-dependent data for potential use in gauging how the reactions leading to the formation of SWNTs might proceed kinetically. We present a photograph that shows overall plume development, and some spectral mea-

* Corresponding author. Fax: +1-281-483-2162; e-mail: c.scott@jsc.nasa.gov

0009-2614/99/$ - see front matter
PII: S0009-2614(99)00098-6

surements taken at various times after the laser pulse, and time-dependent measurements at various wavelengths. Correlations of these spectral data from a parametric study of SWNT production will be presented later.

2. Experiment

The apparatus for nanotube production by laser ablation, shown in Fig. 1, is similar to the one used at Rice University [8], and is described in detail elsewhere [12]. The current configuration uses two 10 Hz pulsed lasers (370 mJ/pulse and 5.5 mm in diameter), one operating at 532 nm (green), followed by the second one operating at 1064 nm (IR) 50 ns later. The graphite target containing cobalt and nickel (1 atom% each) is in a flow tube maintained at 1473 K in a flowing argon atmosphere (100 sccm flow; 66.7 kPa pressure). Light emitted from the plume is transferred via an optical fiber to a Spex 270M spectrograph. Two detectors are used for recording the emission spectra: a gateable intensified charge-coupled device (ICCD) and a photomultiplier tube (PMT). Most of the spectra are recorded with 25 μm slit widths using a 300 line/mm grating blazed at 500 nm. All the spectra are intensity calibrated using a standard lamp the calibration of which is traceable to the NIST.

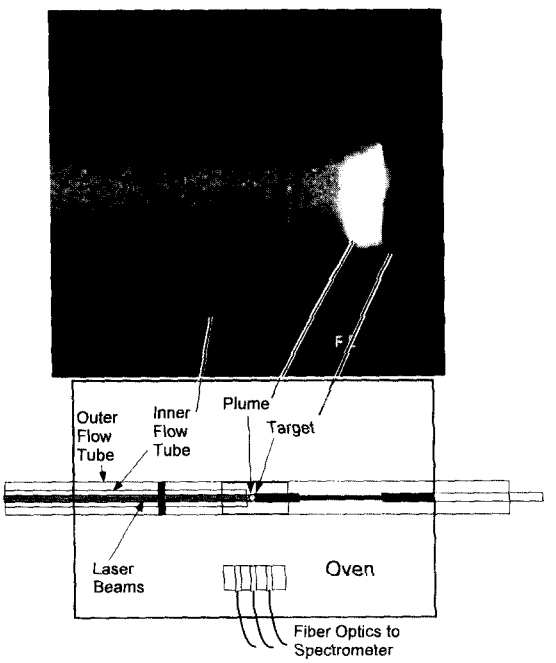

Fig. 1. Photograph of target, plume, and laser-illuminated flow and particles in inner flow tupe with the configuration of the oven and fiber-optic light collectors.

Transient spectral data is collected by connecting the output of the PMT to a transient digitizer with a 10 ns channel width. Time-averaged spectra are collected with gate widths of 10 μs and at different times (0.4, 8 and 25 μs) after the IR laser pulse.

Whereas the lasers scan across the target during a production run, all transient and steady-state data are collected with stationary laser beams fixed at the center of the target. Data collection is initiated 90 s after the start of the laser beams to allow for thermalization of the target surface.

3. Measurements and discussion

3.1. Photographic observations

Photographs such as seen in Fig. 1 were used to obtain estimates of the size and location of the visible plume. The luminous plume appears violet–white and is confined to a small region near the surface of the target. Its duration is less than 1 ms per pulse, as confirmed first by high-speed video and then by transient emission measurements. This photograph was taken with a notch filter to remove scattered 532 nm laser radiation. To the left of the plume, inside the 25 mm inner flow tube, there is a glow that appears to contain high-temperature particles, probably heated to incandescence by the lasers. Our calculations of particle absorption of laser energy (taking into account the complex index of refraction of the particles) show that a large fraction of each particle may vaporize, particularly by the 532 nm beam. The fraction vaporized is independent of particle size, as long as the particles are smaller than the laser wavelength.

3.2. Emission spectral distributions

Spectra averaged over about 10 μs, at delay times of 0.4, 10, and 25 μs after the IR laser pulse, were obtained in the spectral range of about 320–630 nm

(Fig. 2). The predominant feature is the C_2 $d^3\Pi_g$–$a^3\Pi_u$ Swan band emission system [13,14]. To show relative changes in the profiles these spectra are normalized to the peak intensity at 516 nm, which is the $(v',v'') = (0,0)$ bandhead of the C_2 Swan bands. The peaks associated with various vibrational transitions, $\Delta v = v' - v''$, are indicated in Fig. 2, along with a tentative identification of C_3 emission. We do not see any atomic lines in this spectral range.

Comparisons of spectra for various laser pulses and delay times are shown in Fig. 3. We can see that the single laser pulses produce much less radiation than the two lasers together. The effect is more than just additive. There seems to be a synergism in intensity that is consistent with production of carbon SWNTs, where the two-laser-pulse production rate is much greater than the sum of the single-pulse production rates [8]. In Fig. 3 we see that the intensity decreases with time for all laser combinations. This time evolution will be discussed later.

An estimate of the vibrational temperature is obtained from the ratios of vibrational peaks in the spectrum. Using a technique described in Ref. [15], theoretical spectra were calculated at various temperatures, and ratios of integrals over short intensity ranges were found as a function of temperature. In particular we chose to use the ratio of intensity integrals in the vicinity of the vibrational peaks (1,0) and (0,0) of the C_2 Swan band ($d^3\Pi_g$–$a^3\Pi_u$). Integrated intensities over the wavelength ranges 465.04–475.87 nm and 509.87–519.07 nm were determined, with an estimated underlying continuum subtracted. The points at the earliest time cover an interval from 0.4 to 10.4 μs. During that time there is a significant variation in the intensities. Therefore, the inferred temperature during that interval is an approximate average. The temperatures during the first 30 μs, shown in Fig. 5, range from 2500 to 3800 K. Note that the temperatures decrease slowly with time over the range covered and that the temperature is highest with both laser pulses together. The temperatures for the green single pulse is higher than for the IR one.

In an attempt to obtain another estimate of temperatures we compared measured spectra with spectra calculated at various temperatures. We saw no consistent agreement in the shape of the spectral curves for any temperature. If we obtained a good fit for one of the band sequences $\Delta v = 0$, 1, or 2, then the other sequences did not fit well. This implies that there may be significant non-equilibrium in the vibrational levels due, perhaps, to chemiluminescence.

In Figs. 2 and 3 we see an underlying continuum having a maximum at about 400 nm. The underlying

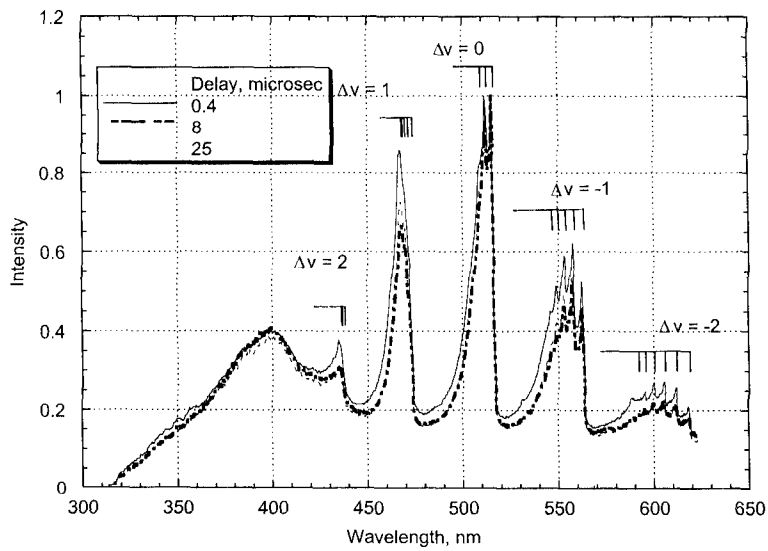

Fig. 2. Normalized spectral distributions obtained in laser ablation plume at various times after laser pulses with identification of peaks associated with C_2 Swan bands and C_3. Both lasers are fired.

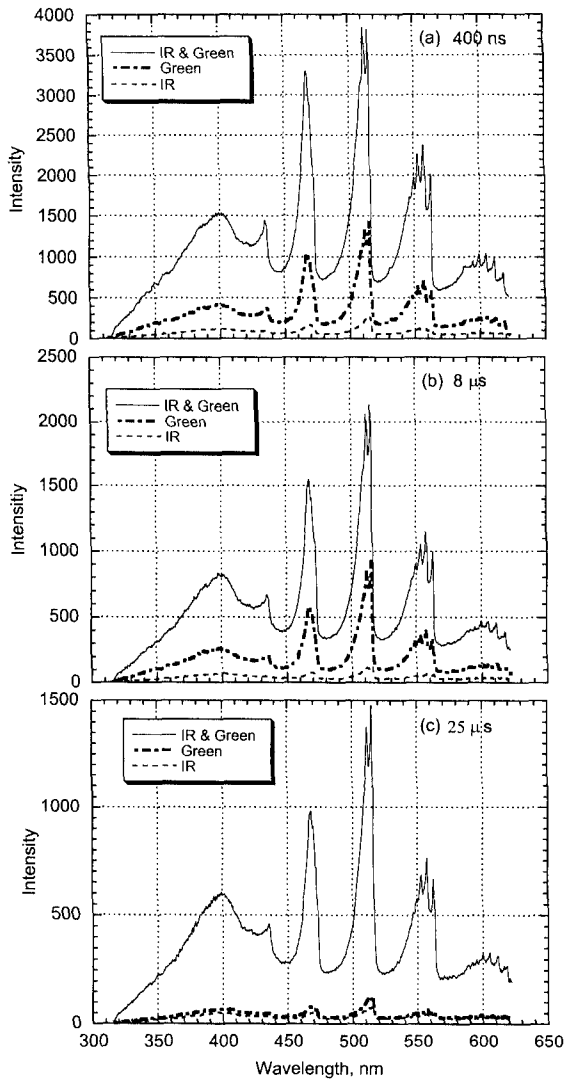

Fig. 3. Un-normalized spectra taken 0.4, 8, and 25 μs after laser pulses for combination and single laser pulses.

continuum may be due to radiation from C_3 and to particulate continua. At short wavelengths it is most likely due to C_3. Rohlfing [16] attributes a similar looking spectrum to Rayleigh emission from particles and to C_2 ($C\,^1\Pi_g$–$A\,^1\Pi_u$), whereas Monchicourt [17] attributes spectra in this region to C_3 (Σ_g^+–Π_u). The measured absorption cross-section profiles of C_3 ($X\,^1\Sigma_g^+$–$A\,^1\Pi_u$) by Cooper and Jones [18] in the temperature range determined here are comparable to our measurements.

The significant continuum underlying the C_2 Swan bands (400–650 nm) is also not well understood. It may be due to particles of carbon and/or catalyst smaller than the wavelength of light. However, the spectral distribution is not understood. We have calculated black-body and Rayleigh particle emission [19] curves, but there does not seem to be a temperature that would yield good agreement over the entire spectral range. It is possible that electrons may be created in the laser ablation plume that recombine to radiate free-bound continua. Calculations were made of C^+–e^- continua for a range of temperatures. These calculations do not seem to support this hypothesis because the spectral distribution is not consistent at low wavelengths at any temperature, with the intensity falling off significantly at short wavelengths.

3.3. Transient emission measurements

Transient measurements of emission at various wavelengths are made with a spectral bandwidth of 6.25 nm to probe the kinetics of plume development. A summary is given in Fig. 4. For each wavelength the intensity is normalized by the maximum value that occurs between 100 and 1200 ns. All wavelengths except those at 350 and 400 nm correspond to peaks in the C_2 Swan band spectrum. The peak at 400 nm, as well as the radiation at 350 nm, may correspond to C_3 and possibly to unresolved cobalt and nickel atomic lines very early in the plume development. Given this, we see a different rate of production and decay of C_3 and Co and Ni as compared with C_2. All of the traces contain some background from particles or other species.

In the first 2.5 μs of the history shown in Fig. 4a, we see the initial transient of the intensities, where the 350 nm measurement shows high relative intensity spike 100 ns after the laser pulse. It is followed by a rise to a peak at 400 ns and then drops quickly to 20% of the peak by 1700 ns. The time that the intensities reach a maximum varies as a function of wavelength. Wavelengths associated with the C_2 Swan bands tend to peak around 800–1100 ns. At an estimated speed of sound of about 1200 m/s (based on a temperature of 4000 K) the distance the plume could travel would be about 1.2 mm. This is consistent with the location of the observation point from the target surface.

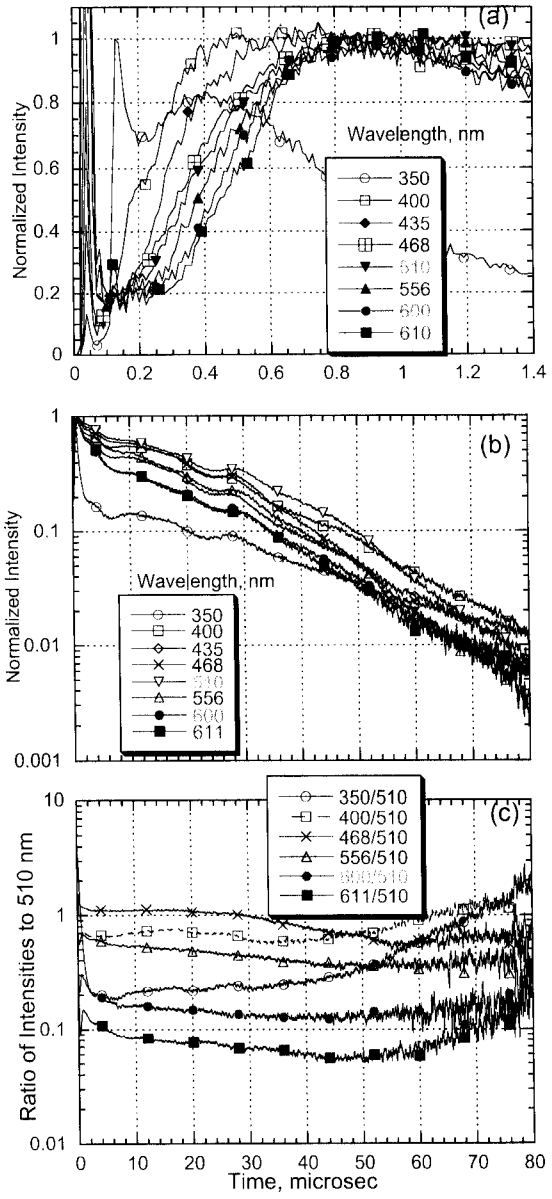

Fig. 4. Transient behavior of laser plume intensities at various wavelengths. (a) Normalized intensities during early transient, (b) normalized and smoothed for period of zero to 80 μs, and (c) ratios of intensities with respect to intensity at 510 nm. The spectral bandwidth is 6.25 nm.

In Fig. 4b we notice that after the initial transient there are three fairly distinct regions of intensity decay for most wavelengths. One region occurs from about 1.6 to 6.0 μs, another from about 12 to 20 μs, and the last appears to be from about 30 to at least 80 μs. Characteristic decay times, determined from curve fits of the transient data over these times, are given in Table 1. The first time period may correspond to chemical reactions and to cooling of the plume. The second probably corresponds to reactions that consume C_2 and C_3. The last period probably is a combination of loss of C_2 and C_3 as well as a drop in particle temperature. Since these decay times are much longer than the radiative lifetimes of the bands, the decay is related to a change in the number and/or temperature of the radiating species. The excited state C_2 and C_3 may be formed from atomic and molecular recombination as well as multi-photon induced dissociation of carbon clusters including fullerenes. Experiments are in progress to verify this

Table 1
Characteristic decay times in microseconds for three regions and eight wavelengths, λ

λ (nm)	1.6–6.0 μs Early reaction zone	12–20 μs Late reaction and cooling zone	30–80 μs Particle cooling zone
350	8.41	30.6	27.6
400	13.2	29.1	17
435	9.31	23.3	16.7
468	12.5	26.3	11.3
510	13.4	27.3	12.3
556	9.29	22.1	12.2
600	6.68	22.1	15.2
611	7.11	20.0	16.0

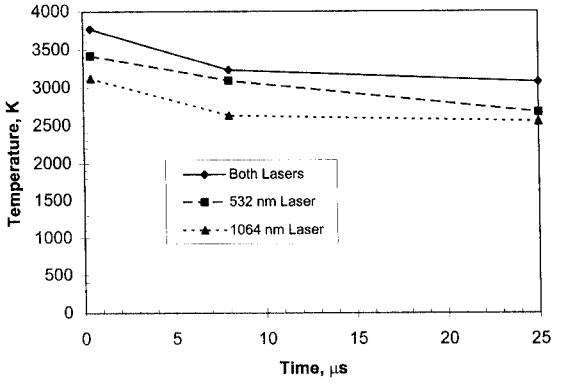

Fig. 5. Temperatures inferred from ratios of intensity integrals with single and double laser pulses.

conjecture and to distinguish these different mechanisms.

In Fig. 4c we see time-dependent ratios of intensities taken at various wavelengths for the span of time up to 80 μs. Variations (humps) seen in the decay (Fig. 4b) in the neighborhood of 10 and 28 μs appear weakly only in the ratios 350/510 and 400/510 because the radiation is from two species. Since we see no perturbations in the ratio associated with various Δv bands of C_2 it is very likely that the temperature does not vary much. The ratio of 468–510 nm is almost constant from 4 μs until about 20 μs, implying that the vibrational temperature is relatively constant during that interval. We see that there was not much variation in temperature during this time period as determined from intensity integral ratios. After 20 μs the ratio decreases until about 55 μs.

The fact that the ratio of intensities of 350/510 nm increases from 7 μs onward is not understood, especially after about 50 μs. It may be associated with a disappearance of C_2 relative to particulates. This same behavior is seen in the ratio of 610 to 510 nm.

4. Conclusions

We have presented the first known optical diagnostics measurements taken in a laser ablation plume during the production of SWNTs. As seen in the photograph the luminous plume is only a few millimeters in diameter and extends a few millimeters from the surface of the target. A glow is seen where the laser illuminates the upstream particles in the flow tube. This is attributed to luminous particles heated by the laser beams.

Spectral measurements of the plume emission indicate that the primary emission is from the C_2 Swan band system. No atomic lines are seen in the wavelength range measured. Additional data collection at shorter times ($\Delta t \sim 0$ ns) and absorption measurements are planned to monitor the atoms. There is also a significant continuum underlying these bands that is probably from particulate radiation. However, the intensity distribution does not clearly indicate that this is gray body radiation. It also deviates from Rayleigh particle emission. We also see a feature in the spectrum that covers a range of 310 nm to at least 430 nm, peaking at about 400 nm which appears to be C_3. No atomic lines are seen in the wavelength range measured. Higher intensities are seen with both laser pulses as compared with only single pulses. This correlated with the amount of SWNTs produced when the two laser pulses are separated in time by 50 ns. Temperatures at several time points are inferred from measured intensity ratios of integrals of Swan band features. The temperatures also showed a dependence on the combination of laser pulses, with the combination of two laser pulses resulting in higher temperatures and the 532 nm laser producing higher temperatures than the 1064 nm laser. The range of temperatures during the first 30 μs was estimated to be from 2500 to 3800 K.

Transient measurements are made at several wavelengths which showed that peak intensities occur at about 800–1100 ns for the C_2 band heads, whereas radiation at 350 nm peaks much earlier, suggesting a quite different phenomenon is causing radiation at this wavelength. The overall shape of the transient curves is similar for the C_2 band heads, and the curves for 350 and 400 nm appear quite different from the others. In fact, the normalized 350 nm curve becomes greater than the others after about 60 μs implying that the C_2 radiation is disappearing, whereas other radiation, e.g., continuum from particles or other species, remains.

In the future, additional spectral analyses will include regions of the spectrum not included in this study, higher-resolution spectra for temperature determinations, and a parametric study to correlate measurements with SWNT production.

Acknowledgements

The authors gratefully acknowledge the contributions of Professor Richard Smalley and Dr. Andrew Rinzler of Rice University, Dr. Lubert Léger, Mr. William Holmes, Dr. Charles Hakes, Mr. Jeremy Jacobs, Dr. Joe Victor, Dr. Larry Lewis, and Dr. Bradley Files.

References

[1] P.M. Ajayan, O. Stephan, Ph. Redlich, C. Coltrex, Nature 375 (1995) 564.

[2] B.I. Yakobson, R.E. Smalley, Am. Sc. 85 (1997) 324.

[3] S. Frank, P. Poncharal, Z.L. Wang, W.A. de Heer, Science 280 (1998) 1744.

[4] A.C. Dillon, K.M. Jones, T.A. Bekkendahl, C.H. Kiang, D.S. Bethune, M.J. Heben, Nature 386 (1997) 377.

[5] S. Iijima, T. Ichihashi, Nature 363 (1993) 603.

[6] D.S. Bethune, C.-H. Kiang, M.S. de Vries, G. Gorman, R. Savoy, J. Vazquez, R. Beyers, Nature 363 (1993) 605.

[7] C. Journet, W.K. Maser, P. Bernier, A. Loiseau, M. Lamy de la Chapelle, S. Lefrant, P. Deniard, R. Lee, J.E. Fischer, Nature 388 (1998) 756.

[8] T. Guo, P. Nikolaev, A. Thess, D.T. Colbert, R.E. Smalley, Chem. Phys. Lett. 243 (1995) 49.

[9] M. Terrones, N. Grobert, J.P. Zhang, H. Terrones, J. Olivares, W.K. Hsu, J.P. Hare, A.K. Cheetham, H.W. Kroto, D.R.M. Walton, Chem. Phys. Lett. 285 (1998) 299.

[10] H.M. Cheng, F. Li, G. Su, H.Y. Pan, L.L. He, X. Sun, M.S. Dresselhaus, Appl. Phys. Lett. 72 (1998) 3282.

[11] M. Yudasaka, T. Komatsu, T. Ichihashi, Y. Achiba, S. Iijima, J. Phys. Chem. B 102 (1998) 4892.

[12] S. Arepalli, C.D. Scott, to be published in the proceedings of the International Conference on Integrated Nano/Microtechnology for Space Applications, Houston, TX, 1–6 November 1998.

[13] L.L. Danylewych, R.W. Nicholls, Proc. R. Soc. London A 339 (1974) 197.

[14] S.S. Harilal, R.C. Issac, C.V. Bindhu, V.P.N. Nampoori, C.P.G. Vallabhan, J. Phys. D, Appl. Phys. 30 (1997) 1703.

[15] C.D. Scott, H.E. Blackwell, S. Arepalli, M.A. Akundi, J. Thermophys. Heat Transfer 12 (1998) 457.

[16] E.A. Rohlfing, J. Chem. Phys. 89 (1988) 6103.

[17] P. Monchicourt, Phys. Rev. Lett. 66 (1991) 1430.

[18] D.M. Cooper, J.J. Jones, J. Quant. Spectrosc. Radiative Transfer 22 (1979) 201.

[19] C.F. Bohren, D.R. Huffman, Absorption and Scattering of Light by Small Particles, John Wiley, New York, 1993.